Friction and wear performance of an aluminium alloy in artificial seawater

H-Y Ding[1,2*], **G-H Zhou**[1], and **D Hui**[2]
[1]Faculty of Mechanical Engineering, Huaiyin Institute of Technology, Huaian, Jiangsu, People's Republic of China
[2]Department of Mechanical Engineering, University of New Orleans, New Orleans, Louisiana, USA

The manuscript was received on 14 March 2010 and was accepted after revision for publication on 25 October 2010.

DOI: 10.1177/13506501JET811

Abstract: The corrosion wear behaviours of an aluminium alloy 2024Al flat specimen against a 440C stainless-steel counter ball specimen were evaluated in artificial seawater by using a ball-on-flat configuration with 300 μm amplitude at room temperature for 1 h. Reference experiments were also performed in distilled water. The worn surface of the specimen was observed using scanning electron microscopy. The three-dimensional morphology and wear volume loss were determined using a non-contact optical profilometer. Potentiodynamic anodic polarization was used to measure the corrosion behaviours of 2024Al before and after the corrosion wear test. The influences of the aqueous medium on the corrosion resistance, coefficient of friction, and wear loss were analysed. Results show that 2024Al exhibits a dominant pitting corrosion mechanism in seawater and corrosion is accelerated by wear. Seawater can reduce the friction coefficient, whereas the wear loss in seawater is higher than that in distilled water, which can be attributed to a higher Cl^- percentage. This implies that the wear is accelerated by corrosion. There is a positive synergism between corrosion and wear for 2024Al sliding in seawater. The wear mechanism of 2024Al is dominant corrosion fatigue in seawater due to the distinct electrochemical reaction. The profile of wear concave gradually changes from 'V' shape into 'U' shape with the increase of load or frequency.

Keywords: corrosion wear, aluminium, synergism, seawater

1 INTRODUCTION

For its excellent properties of high specific strength, good formability, and good corrosion resistance, aluminium alloy is widely applied in the aerospace and marine [**1**]. In the past years, a lot of studies had been conducted on the corrosion resistance of aluminium alloy in sodium chloride, acid, alkaline solutions [**2**–**6**], and rainwater [**7**, **8**], as well as its tribological and fatigue behaviours [**9**–**12**]. Wear inevitably occurs during the working process of the component. When working in a corrosive medium, wear corrosion occurs. Wear corrosion involves mechanical and chemical mechanisms, the combination of which often results in significant mutual effects because of the complicated synergy (i.e. wear is accelerated by corrosion or vice versa), and both will accelerate the surface damage of materials [**13**].

It is well known that military aircraft often fly from offshore platform or airplane carrier. Aluminium alloy, especially 2024Al, is widely used to make framework, rivet, and propeller blade in the aircraft and marine vessel which may be subjected to wear corrosion caused by seawater and sea-salt spray. Although some researches had been conducted on slurry erosion–corrosion, abrasive-corrosion wear, and cavitation erosion–corrosion behaviours [**14**–**16**], the wear corrosion property of aluminium alloy in seawater has not yet been investigated in detail. Seawater is a natural electrolyte. Most of the elements that can be found on the Earth are present in seawater, at least in trace amounts. When the passive state is locally destroyed in the wear process, the corrosive ions in seawater can erode into the defects and change the friction behaviours of the materials [**17**, **18**], mostly accelerating the wear process [**19**].

*Corresponding author: Faculty of Mechanical Engineering, Huaiyin Institute of Technology, 1 Meicheng Road, Huaian, Jiangsu 223003, People's Republic of China.
email: nanhang1227@gmail.com; nanhang1227@yahoo.com.cn

This work was undertaken to study, in a detailed manner, the performance of wear corrosion experiments for 2024Al in seawater. With the reference experiments performed in distilled water, the influence of corrosive medium on the friction behaviour and the synergism between corrosion and wear were evaluated.

2 EXPERIMENTAL PROCEDURE

2.1 Materials

The aluminium alloy 2024Al (0.50 per cent Si plus Fe, 4.0 per cent Cu, 0.50 per cent Mn, 1.40 per cent Mg, 0.30 per cent Zn, and balance Al) with hardness of 177 HV was cut into 20 mm×18 mm×4 mm rectangular specimen by using the electrical discharge method. It was then ground to an average surface roughness of $R_a = 1.2\,\mu$m and was mounted on the table as the lower specimen. Commercially available 440C stainless steel (ø4 mm) with hardness of 610 HV was used as the upper mating ball and was kept stationary.

2.2 Experiment details

Almost all the elements that can be found on the Earth are present in seawater. However, 11 of the constituents alone account for 99.95 per cent of its total solutes, chloride ions being the largest constituent. Artificial seawater with a pH of 8 was synthesized in the laboratory according to the composition presented in Table 1.

An immersion corrosion test in seawater was conducted to evaluate the corrosion property of 2024Al. After being abraded with SiC paper (2000 grit), the 2024Al block was put into seawater for 168 h at room temperature. It was then ultrasonically cleaned in ethanol and dried for further morphological observation and electrochemical measurement.

All the wear experiments were performed using a ball-on-flat reciprocal tribometer UMT-2 (CETR, USA). Prior to each wear test, the steel ball and 2024Al specimen were ultrasonically cleaned in acetone for 10 min and then air dried. The wear experiments were performed at room temperature in distilled water and artificial seawater with the same concentration as used in the immersion corrosion test. Each test was carried out for 1 h with reciprocating amplitude of 300 μm imposed by the tribometer. The normal load was in the range of 0.5–2 N, and the sliding frequency varied in the range of 5–20 Hz. The aqueous solution was added into the rubbing zone till full of the contact area every 20 min using an injection tube. The coefficient of friction was obtained directly from the tribometer. After the completion of the wear test, 2024Al specimen was ultrasonically cleaned in acetone. Later, their surface characteristics and electrochemical properties were investigated. Three replicate tests were conducted for each wear condition.

Table 1 Composition of artificial seawater

Solute	Concentration (g/kg)
NaCl	26.726
$MgCl_2$	2.26
$MgSO_4$	3.248
$CaCl_2$	1.153
$NaHCO_3$	0.198
KCl	0.721
NaBr	0.058
H_3BO_3	0.058
Na_2SiO_3	0.0024
H_3PO_4	0.002
Al_2Cl_6	0.013

To illustrate the influence of wear and immersion on corrosion, 2024Al specimens in three different states were electrochemically tested.

1. The sample without corrosion or wear was electrochemically tested in seawater (original sample).
2. The sample without wear was immersed in seawater for 168 h and was then electrochemically tested (after immersion).
3. The sample without corrosion or wear underwent wear in seawater and was then electrochemically tested (after corrosion wear).

2.3 Measurement and characterization

Electrochemical measurements were carried out at room temperature using a CHI760B potentiostat/galvanostat system with a three-electrode cell. The specimen was used as the working electrode. A platinum plate and saturated calomel electrode (SCE) were used as the counter and reference electrodes, respectively. A dynamic scan from −1.5 to +1.5 V (SCE) at a potential scanning rate of 0.1 mV/s was performed in seawater. Potentiodynamic anodic polarization curves were automatically acquired. The corrosion potential (E_{corr}) and corrosion current density (i_{corr}) were calculated by software using the*Tafel extrapolation method*.

The morphology of the corrosive surface and wear scar was observed using a HITACHI 3000N scanning electron microscope (SEM). The three-dimensional (3D) morphology, the profile across the centre, and the wear volume loss of the wear scar were investigated using a Micro-XAM non-contact optical profilometer (ADE, USA).

3 RESULTS AND DISCUSSION

3.1 Corrosion properties of 2024Al in seawater

The corrosion images of 2024Al after 168 h immersion in seawater are given in Fig. 1. Many widely scattered corrosion pits were observed on the surface of

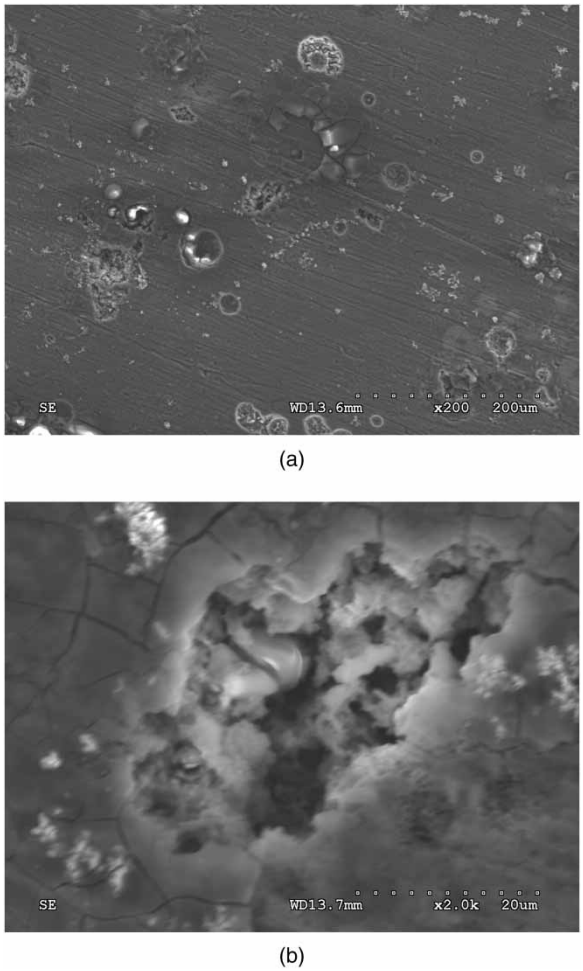

Fig. 1 SEM photographs of 2024Al aluminium alloy after immerging in seawater: (a) at low-magnitude scale and (b) at high-magnitude scale

the sample, as evident in Fig. 1(a). Figure 1(b) shows a distinguished pit larger than 20 μm. This indicates a worse corrosion property and a dominant pitting corrosion mechanism of 2024Al in seawater.

Seawater, by virtue of its chloride content, is an efficient electrolyte. Aluminium is sensitive to Cl^- ions due to the strong destructive action of Cl^- on the passive films of aluminium [**20**, **21**]. Previous studies showed that although it is difficult to form a diffluent chloride corrosion product, some Cl^- ions would still be adsorbed into the corrosion layer and be present as $AlCl_3$, and would react from $Al(OH)_3$ via a series of the chloridizing process [**22**, **23**]

$$Al(OH)_3 + Cl^- \rightarrow Al(OH)_2Cl + OH^- \quad (1)$$

$$Al(OH)_2Cl + Cl^- \rightarrow Al(OH)Cl_2 + OH^- \quad (2)$$

$$Al(OH)Cl_2 + Cl^- \rightarrow AlCl_3 + OH^- \quad (3)$$

The solution composition in the pitting pore is obviously different from that of the bulk [**24**]; a higher OH^- concentration outside the pitting pore results in higher acidity in the pitting pore. The pitting corrosion is consequently enhanced.

3.2 Synergism of corrosion on wear

In the case of the load of 2 N, the frequency versus coefficient of friction and wear volume loss of 2024Al sliding against the 440C stainless-steel ball in distilled water and seawater are illustrated in Fig. 2. Generally, the coefficient of friction decreases with the increase of the frequency in both solutions. Furthermore, the coefficient in seawater is always smaller than that in distilled water no matter what frequency it is. The maximum difference is observed at a frequency of 15 Hz, where the coefficient of friction in seawater is 47 per cent smaller than that in distilled water. This indicates a remarkable anti-friction effect of seawater.

At fixed sliding amplitude, a higher frequency results in a more rapid sliding velocity. Owing to the repetitive tangent stress, it is easier to generate granular debris at a higher sliding speed. Meanwhile, the actual sliding amplitude is so small that it is impossible for tiny debris to be completely expelled from the wear contact area. With the aid of a flowing aqueous solution, the trapped debris may act as rolling balls. The debris wrapped by the lubricative seawater can change the two-body friction into three-body friction. This results in a much smoother wear process. Therefore, the coefficient of friction generally decreases with an increase of the frequency in both the aqueous solutions.

Active elements such as S, P, and Cl are all present in seawater in the form of sodium chloride, calcium chloride, magnesium sulphate, etc. Owing to the friction heat generated during the friction process these elements will react with the element Fe in the 440C ball, and an easy-shear tribo-layer containing ferric sulphide, ferric phosphate, and ferric chloride forms. The metal-to-metal contact is thereby separated by this film. Accordingly, the coefficient of friction decreases in seawater compared to that in distilled water.

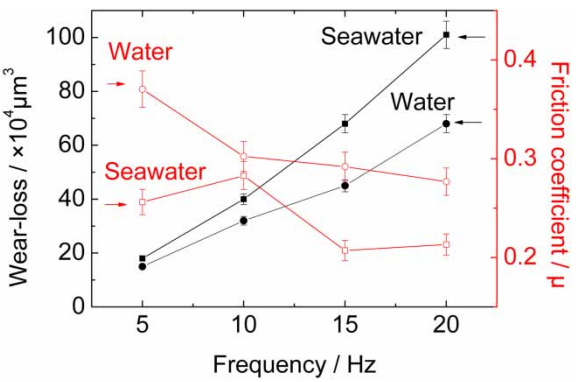

Fig. 2 Coefficient of friction and wear loss of 2024Al. The dotted line and solid line correspond to the coefficient of friction and wear loss, respectively

From the wear-loss curves in Fig. 2, one can also see that the wear loss is always greater in seawater than that in distilled water, and the higher the frequency, the larger the difference. It is about 48 per cent greater in seawater compared to that in distilled water when sliding at a frequency of 20 Hz. These results strongly suggest that wear is accelerated by corrosion.

3.3 Synergism of wear on corrosion

Synergism between corrosion and wear is composed of the effect of wear on corrosion and the effect of corrosion on wear. To reveal the effect of wear on corrosion, electrochemical tests were conducted on 2024Al with different states. Corrosion by aqueous solution is an electrochemical process; all metals and alloys have a specific electrical potential at a specific level when in contact with seawater. Figure 3 shows the typical anodic potentiodynamic polarization curves of 2024Al in three different states. The corrosion potential (E_{corr}) and corrosion current density (i_{corr}) are summarized in Table 2.

It should be noticed that typical passivation behaviour is clearly observed for 2024Al in all the three states in seawater (i.e. the electrode) is anodically polarized to a more positive potential, whereas the value of the corresponding current remains limited. The polarization curves of 2024Al shift towards the positive direction compared to the original sample after both the corrosion wear and immersion test.

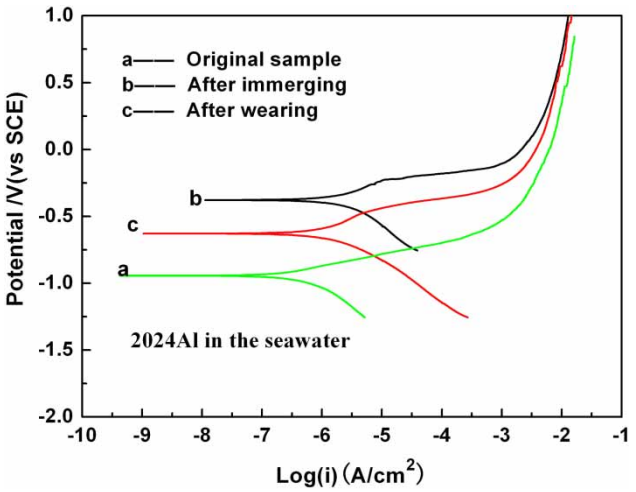

Fig. 3 Polarization curves of 2024Al in seawater

Table 2 Results of polarization experiments of 2024Al in seawater

State	Corrosion potential (V)	Corrosion current density (A/cm^2)
Original sample	−0.930	2.82×10^{-7}
After immersion	−0.378	2.30×10^{-6}
After corrosion wear	−0.622	1.18×10^{-6}

This can be identified as a trend of reduced corrosion. In the authors' interpretation, the nascent aluminium can react with oxygen or water and it forms a coherent surface oxide which impedes further reaction of aluminium with seawater. However, the i_{corr} of 2024Al after corrosion wear in seawater increases 76 per cent compared to that of the original sample, implying a markedly increased corrosion speed. This exactly confirms that corrosion in seawater is accelerated by wear.

From the anode polarization curve of the 2024Al sample after wear it can be seen that the passivation region is generated at −0.42 V. Previous study [**25**] showed that the passive film of 2024Al formed at negative potential is a hydrated oxide film with high porosity and low relative density. This brittle film is mainly composed of γ-Al_2O_3. It can be easily disintegrated or removed by the action of the rapid tribo-ball during the wear process. This assumption is also supported by SEM photograph of the unbroken brittle film around the wear scar of 2024Al in seawater, shown in Fig. 4.

Local degradation is easier to occur on the surface of 2024Al attributable to the uneven passive film induced by the defects of mechanical cracks, abrasion, impurity, dislocations, and cavities during the wear process [**26**]. This would improve both the corrosion current and the desquamating speed of the worn 2024Al, and lead to a worse corrosion wear property. The synergistic effect of corrosion on wear is consequently increased. The wear is thus significantly increased in seawater by the tribo-corrosion interactions. Meanwhile, corrosion in seawater is accelerated by wear as mentioned above. Therefore, 2024Al exhibits a positive synergism between corrosion and wear in seawater.

3.4 Influence of medium on the wear mechanism

Figure 5 depicts SEM images of wear scars in seawater after cleaning. The width of the wear scar is a

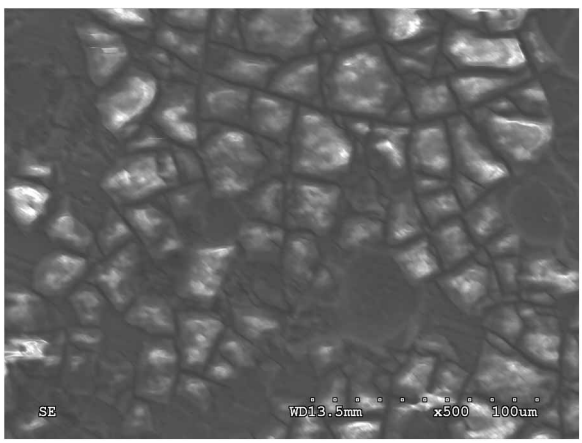

Fig. 4 SEM photograph of the brittle film at the edge of the wear scar of 2024Al in seawater

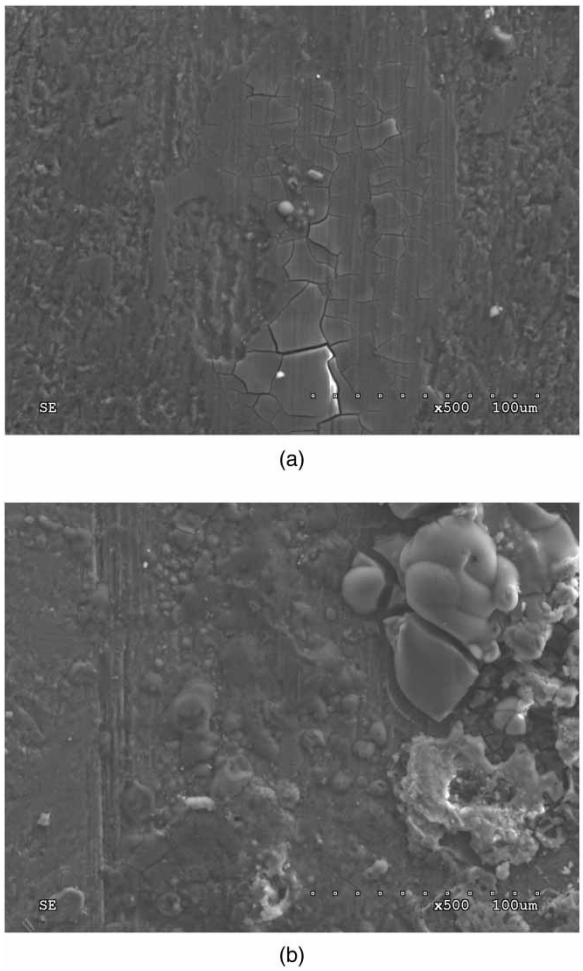

Fig. 5 SEM photographs of 2024Al wear scars in seawater: (a) at 1 N–10 Hz and (b) at 1.5 N–20 Hz

little shallower at lower load. Besides some dull micro-cutting signs, many micro-cracks were generated in seawater, either parallel or perpendicular to the friction direction, most of which were connected and can desquamate at any time, as shown in Fig. 5(a). This demonstrates the brittle passivation film mentioned above. While the load or frequency increases some corrosion tumours are obviously present on the wear scar; these corrosion products have weak bonding forces with the matrix and would form tiny debris during the friction process. It may be assumed that electrochemical reaction between the aluminium alloy and seawater occurred. Accordingly, the wear loss of 2024Al

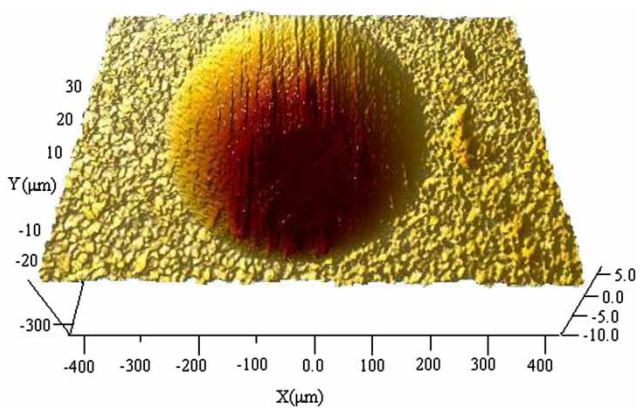

Fig. 6 Three-dimensional morphology of the cleaned wear scar of 2024Al

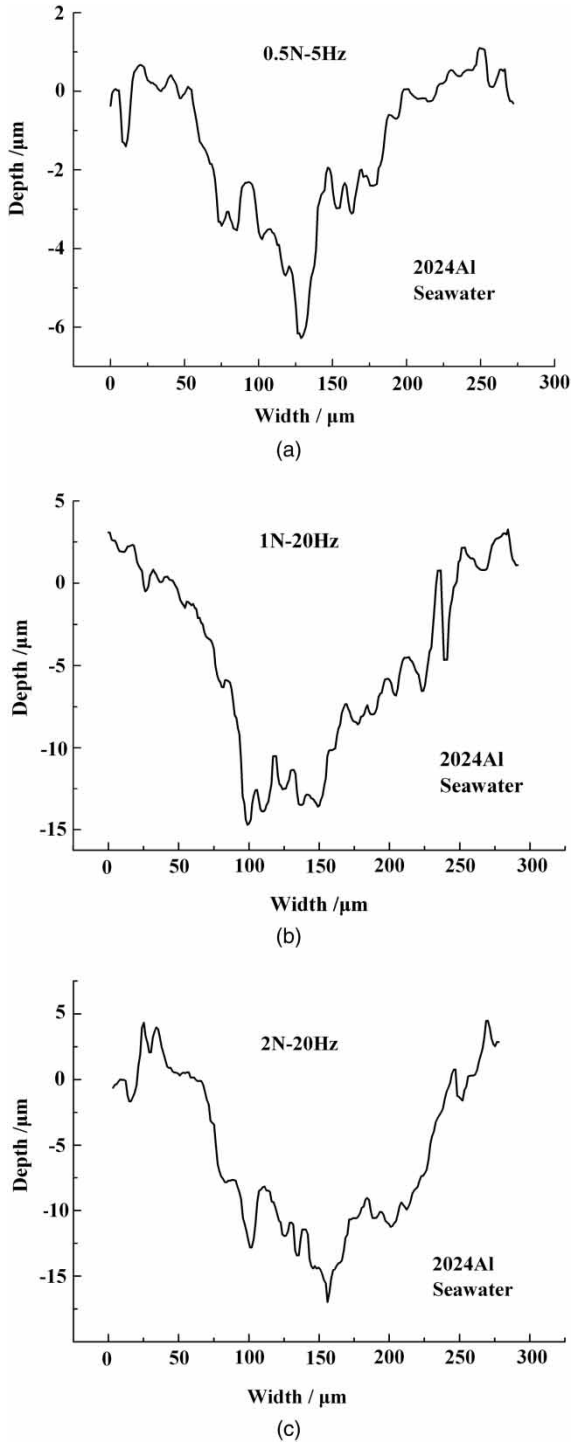

Fig. 7 Cross-sectional profile curves of wear scars in seawater: (a) at 0.5 N–5 Hz; (b) at 1 N–20 Hz; and (c) at 2 N–20 Hz

consisted of the delamination of brittle film, debris, and the corrosion product. Thus, the wear mechanism of 2024Al is mainly the dominant corrosion fatigue in seawater.

All the wear scars of 2024Al in distilled water and seawater have the same typical regular concave illustrated in Fig. 6. It presents typical shallower 'V' shape at lower load, the width and depth get larger with the increasing of load or frequency, and the profile of concave gradually changes into 'U' shape (Fig. 7). It can be seen from Fig. 7 that there are asperities, caused by the harder mating ball, at the edge of each concave profile. The weak plow effect results in such small plastic deformation. Furthermore, all the concaves are in relative smooth states without suddenly changing slot, implying a reaction of tribo-chemical. The 3D morphology and cross-sectional profile reinforce the assumption of corrosion fatigue wear mechanism deduced by SEM.

4 CONCLUSION

The immersion corrosion test demonstrates a dominant pitting corrosion mechanism for 2024Al in seawater. A series of ball-on-flat wear tests were carried out in distilled water and seawater at different loads and frequencies. The coefficient of friction of the 2024Al/440C tribo-pair generally decreases with an increasing frequency in both the aqueous solutions. Furthermore, the coefficient is always smaller in seawater than that in distilled water, and therefore exhibits remarkable anti-friction function in seawater. The wear loss in seawater is higher than that in distilled water due to the corrosion effect of Cl^- ions on the 2024Al substrate; meanwhile, corrosion speed of 2024Al after corrosion wear is increased, and thus presents a positive synergism ratio between corrosion and wear. The wear mechanism of 2024Al is typically corrosion fatigue in seawater due to distinct electrochemical reactions. The profile of concave gradually changed from 'V' shape into 'U' shape with the increase of load or frequency.

ACKNOWLEDGEMENT

This work is supported by Jiangsu key Laboratory of friction wear opening Foundation under grant no. kjsmcx07003 and Qing Lan project 2010.

REFERENCES

1 **Miller, W., Zhuang, S. L., Bottema, J., Wittebrood, A. J., Smet, P. De, Haszler, A.,** and **Vieregge, A.** Recent development in aluminium alloys for the automotive industry. *Mater. Sci. Eng. A*, 2000, **280**, 37–49.

2 **Oguzie, E. E.** Corrosion inhibition of aluminium in acidic and alkaline media by Sansevieria trifasciata extract. *Corros. Sci.*, 2007, **49**, 1527–1539.

3 **Garrigues, L., Pebere, N.,** and **Dabosi, F.** An investigation of the corrosion inhibition of pure aluminum in neutral and acidic chloride solutions. *Electrochim. Acta*, 1996, **41**, 1209–1215.

4 **Shao, M. H., Fu, Y., Hu, R. G.,** and **Lin, C. J.** A study on pitting corrosion of aluminum alloy 2024-T3 by scanning microreference electrode technique. *Mater. Sci. Eng. A*, 2003, **344**, 323–327.

5 **Szklarska-Smialowska, Z.** Pitting corrosion of aluminium. *Corros. Sci.*, 1999, **41**, 1743–1767.

6 **de la Fuente, D., Otero-Huerta, E.,** and **Morcillo, M.** Studies of long-term weathering of aluminium in the atmosphere. *Corros. Sci.*, 2007, **49**, 3134–3148.

7 **Lakshmi Priya, S., Chitra, A., Rajendran, S.,** and **Anuradha, K.** Corrosion behaviour of aluminium in rain water containing garlic extract. *Surf. Eng.*, 2005, **21**, 229–231.

8 **Ross W. S.** Kinetic aspects of aqueous aluminum chemistry: environmental implications. *Coord. Chem. Rev.*, 1996, **149**, 81–93.

9 **Bussu, G.** and **Irving, P. E.** The role of residual stress and heat affected zone properties on fatigue crack propagation in friction stir welded 2024-T351 aluminium joints. *Int. J. Fatigue*, 2003, **25**, 77–88.

10 **Chen, Y. K., Han, L., Chrysanthou, A.,** and **O'Sullivan, J. M.** Fretting wear in self-piercing riveted aluminium alloy sheet. *Wear*, 2003, **255**, 1463–1470.

11 **Wang, L. L., Cai, J. Q., Zhou, J.,** and **Duszczyk, J.** Characteristics of the friction between aluminium and steel at elevated temperatures during ball-on-disc tests. *Tribol. Lett.*, 2009, **36**, 183–190.

12 **Elliott III, C. B.** and **Hoeppner, D. W.** The importance of wear and corrosion on the fretting fatigue behavior of two aluminum alloys. *Wear*, 1999, **236**, 128–133.

13 **Fedrizzi, L., Rossi, S., Bellei, F.,** and **Deflorian, F.** Wear-corrosion mechanism of hard chromium coatings. *Wear*, 2002, **253**, 1173–1181.

14 **Li, Y., Burstein, G. T.,** and **Hutchings, I. M.** The influence of corrosion on the erosion of aluminium by aqueous silica slurries. *Wear*, 1995, **186–187**, 515–522.

15 **Meyer-Rodenbeck, G., Hurd, T.,** and **Ball, A.** On the abrasive-corrosive wear of aluminium alloys. *Wear (Switzerland)*, 1992, **154**, 305–317.

16 **Kassner, M. E.** and **Hayes, T. A.** Creep cavitation in metals. *Int. J. Plast.*, 2003, **19**, 1715–1748.

17 **Ponthiaux, P., Wenger, F.,** and **Drees, D.** Electrochemical techniques for studying tribocorrosion processes. *Wear*, 2004, **256**, 459–468.

18 **Koa, P. L., Wozniewskib, A.,** and **Zhou, P. A.** Wear-corrosion-resistant materials for mechanical components in harsh environments. *Wear*, 1993, **162**, 721–732.

19 **Jiang, J., Stack, M. M.,** and **Neville, A.** Modelling the tribocorrosion interaction in aqueous sliding conditions. *Tribol. Int.*, 2002, **35**, 669–679.

20 **Ambat, R.** and **Dwarakadasa, E. S.** Studies on the influence of chloride ion and pH on the electrochemical behavior of aluminum alloys 890 and 2014. *J. Appl. Electrochem.*, 1994, **24**, 911–916.

21 **Brett, C. M. A.** The application of electrochemical impedance techniques to aluminum corrosion in

acidic chloride solution. *J. Appl. Electrochem.*, 1990, **20**, 1000–1003.

22 **Liepina, L.** and **Kadek, V.** Conditions for disruption of the primary film during corrosion of aluminum in netural solutions. *Corros. Sci.*, 1966, **6**, 177–181.

23 **Nguyen, T. H.** and **Foley, R. T.** The chemical nature of aluminum corrosion. *J. Electrochem. Soc.*, 1980, **127**, 2563–2570.

24 **Edeleanu, C.** and **Evans, U. R.** The causes of the localized character of corrosion on aluminium. *Trans. Faraday Soc.*, 1951, **47**, 1121–1135.

25 **Nahar, R. K.** Study of the performance degradation of thin film aluminum oxide sensor at high humidity. *Sens. Actuators B*, 2000, **63**, 49–54.

26 **Zhang, T. C., Jiang, X. X.,** and **Li, S. Z.** Acceleration of corrosive wear of duplex stainless steel by chloride in 69% H_3PO_4 solution. *Wear*, 1996, **199**, 253–259.